

IN-90-412

032475

Global evolution of solid matter in turbulent protoplanetary disks

I. Aerodynamics of solid particles

T.F. Stepinski¹ and P. Valageas²¹ Lunar and Planetary Institute, 3600 Bay Area Blvd., Houston, TX 77058, USA² Service de Physique Théorique, CEN Saclay, F-91191 Gif-sur-Yvette, France

Received 9 May 1995 / Accepted 18 September 1995

Abstract. The problem of planetary system formation and its subsequent character can only be addressed by studying the global evolution of solid material entrained in gaseous protoplanetary disks. We start to investigate this problem by considering the space-time development of aerodynamic forces that cause solid particles to decouple from the gas. The aim of this work is to demonstrate that only the smallest particles are attached to the gas, or that the radial distribution of the solid matter has no momentary relation to the radial distribution of the gas. We present the illustrative example wherein a gaseous disk of $0.245 M_{\odot}$ and angular momentum of $5.6 \times 10^{52} \text{ g cm}^2 \text{ s}^{-1}$ is allowed to evolve due to turbulent viscosity characterized by either $\alpha = 10^{-2}$ or $\alpha = 10^{-3}$. The motion of solid particles suspended in a viscously evolving gaseous disk is calculated numerically for particles of different sizes. In addition we calculate the global evolution of single-sized, noncoagulating particles. We find that particles smaller than 0.1 cm move with the gas; larger particles have significant radial velocities relative to the gas. Particles larger than 0.1 cm but smaller than 10^3 cm have inward radial velocities much larger than the gas, whereas particles larger than 10^4 cm have inward velocities much smaller than the gas. A significant difference in the form of the radial distribution of solids and the gas develops with time. It is the radial distribution of solids, rather than the gas, that determines the character of an emerging planetary system.

Key words: accretion disks – solar system: formation

1. Introduction

The combination of observational evidence with theoretical concepts strongly suggests that planetary systems, other than our solar system, ought to exist. We believe that planets form by the accumulation of solid matter¹ in *accretion* disks around young

¹ More precisely, the nonvolatile component of planets. Giant planets, like Jupiter, formed as solid bodies to which a large amount of gas was subsequently added.

low-mass stars. Thus, the seeds of the future planetary system architecture are to be found in the radial distribution of solids. Starting with this paper we embark on an investigation aimed at calculating the time and space evolution of solid material in protoplanetary disks.

It is very important to realize that the distribution of solid particles undergoes a global time evolution, which accompanies, but is not identical to, the global time evolution of the gaseous component of the disk. The gaseous disk spreads and its mass diminishes due to viscous torques. Initially, the solid particles are very small, so they are coupled to the gas, and both components evolve more or less concurrently. With time the solid particles gain mass due to the process of coagulation and decouple from the gas. The subsequent global evolution of solids differs from the evolution of the gas, the divergence being a function of coagulation process time scales and the magnitude of solid-gas interactions. Eventually, as the density of the gas decreases and the mass of solid particles increases, the radial distribution of solids *converges* to its final form. This final form is a major factor in determining the character of the nascent planetary system, inasmuch as any further redistribution of mass is only due to the planet formation process via the growth of planetesimals into protoplanets (Safronov 1969; Greenberg et al. 1978; Kaula 1979; Wetherill 1980; Nakagawa et al. 1983). Although this last process radically changes solid mass distribution on the small-scale, it does not much alter the *average* large-scale radial distribution of solid material.

To begin our discussion we elucidate the two essential concepts underlying our approach. First, we assume that protoplanetary disks are indeed accretion disks and that the accretion process is due to an anomalous viscosity. Astronomical observations of young low-mass stars have led to wide acceptance of the idea that these stars are surrounded by *accretion* disks (for recent reviews see Strom & Edwards 1993; Beckwith 1994). On the other hand, it seems that much of our solar system's gross architecture has arisen from physical processes and conditions characteristic for accretion disks (Levy 1993). Because we believe that the gaseous solar nebula from which the solar system evolved exemplifies contemporaneously observed

disks around low-mass young stars, we can make a persuasive case that *all* protoplanetary disks are in fact accretion disks. The conjecture is that some sort of anomalous viscosity operates in those disks. That is not necessary so, inasmuch as other processes such as centrifugally driven winds (Pudritz & Norman 1983) may cause an accretion of mass as well. Nevertheless, we adopt here the "classical" viewpoint that accretion disks are powered by viscosity created by the interaction of turbulent eddies. We do not specify the source of this turbulence, but instead use the usual α parameterization introduced by Shakura & Sunyaev (1973).

Second, we accept the current planet formation concept according to which planets form by the accumulation of solid matter, beginning with dust, into progressively more massive particles, and eventually culminating in the few large bodies that comprise the planetary system (for a review see Weidenschilling 1988). This is because, in the presence of turbulence, the formation of planets could not have occurred as a result of gravitational instability as was envisioned (Goldreich & Ward 1973) before the accretional (and by conjecture turbulent) character of protoplanetary disks was fully appreciated. In a hypothetical quiescent disk the metamorphosis of fine dust into roughly 1 – 10 km sized solid planetesimals occurs almost instantaneously once the dust layer becomes thin enough for gravitational instability to take place. Thus the radial mass distribution of planetesimals directly reflects the radial distribution of the gas at the moment when the instability occurred. In a turbulent disk no such instantaneous aggregation of solids is possible. Instead, planetesimals are the final product of a relatively long-lasting process of solid material accumulation. Because the solid particles are suspended in a permeating body of moving gas, they undergo radial transport while coagulating into progressively larger particles. Thus the radial mass distribution of planetesimals emerging from a turbulent disk does not reflect the radial distribution of gas at any particular epoch. In order to calculate the radial mass distribution of planetesimals, we have to follow the concomitant evolution of gaseous and solid components of a disk.

Note that once both concepts presented above are accepted, and the coagulation time scale is not very short compared to the viscous time scale², the above conclusion regarding the manner of calculating the mass distribution of planetesimals is unequivocal. However, although both of our principal concepts are favored by theory and observation, the notion that the radial mass distribution of planetesimals can be obtained directly from the surface density of gas (or *vice versa* as in so-called minimum mass solar nebula models) lingers in the literature.

It is quite clear that an understanding of the global evolution of solid particles requires daunting calculations. Before entering into such calculations we need to see a way through some of the potential pitfalls. The first problem is the choice of the starting time and the choice of initial conditions. The processes leading

to the accumulation of solids may, in principle, occur already in a parent molecular cloud even before a cloud collapses to form a star and a disk (Weidenschilling & Ruzmaikina 1994). However, it seems most reasonable to choose the onset of the disk's viscous stage as the starting time for our considerations. The initial conditions for the subsequent disk evolution should be chosen to reflect conditions at the onset of the viscous stage. Because such conditions are poorly constrained, we would start from some arbitrary initial distribution of the surface density of the gas, restrained only by the values of the total mass, M_{disk} , and the total angular momentum, J_{disk} . Fortunately, the specific form of initial conditions does not much influence the evolution of the gas, inasmuch as the process is diffusive in nature and the initial conditions are forgotten after a time short in comparison with the evolutionary time scale. As for solid particles, we assume a certain initial size distribution. The initial space distribution of a solid matter follows the initial surface density of the gas. The subsequent evolution of solid material is *not* a viscous process, and there is a danger that the radial distribution of solids at later times is susceptible to the arbitrariness of the initial conditions. This problem is avoided if the solids are coupled to the gas during the time the gaseous component needs to forget the initial conditions.

The second problem is the desired accuracy in describing the gas-solid interactions. Obviously, we have to consider aerodynamic forces exerted on the solids by the gas because this is the only process leading to the radial evolution of disk's solid material. However, we neglect all potential effects the presence of solids may have on the evolution of the gas. The major effect of solid particles on the evolution of the gas is through the opacity. In the protoplanetary disk the opacity is dominated by solids (dust grains). As the solids evolve due to coagulation and radial transport, so should the opacity (Morfill 1988). This effect is disregarded in our approach and the constant size distribution of dust is used as a parameter needed to calculate the opacity. Such an approach may, nevertheless, provide a reasonable approximation to a disk's opacity as long as there is some amount of small grains well mixed with the gas. Our reasoning is that the coagulation process is not 100% efficient, leaving behind enough small grains to support the opacity. The second effect of solid particles on the evolution of the gas is the gas-solid friction, which is usually negligible compared to other forces acting on the gas, and its omission is justifiable.

The third problem arises because solid particles may either appear or disappear due to thermal processes. The temperature in the disk changes rapidly with the distance from the star. In addition, the entire disk cools down with time. The particles traveling inward may evaporate and new particles condense in regions that just cooled below a certain temperature. Particles with high velocities with respect to the gas may be obliterated by the heat generated by the friction even if the temperature of the ambient gas is low. The difficulty of keeping track of these processes is magnified by the compositional variety of solid particles, which may consist of "rock," "metal," or "ice," as well as the combination of these basic elements. Because our intention is to concentrate on radial motion and coagulation as

² Both coagulation and viscous time scales are neither global nor constant. What we need to compare here are local and momentary values of these time scales.

the two fundamental processes governing the global evolution of solids, we neglect all above mentioned thermal processes. Thus, at least at this stage of our investigation, the solid particles are thermally indestructible, and no new particles can be created.

This concludes the overall description of the approach we have taken to calculate the global evolution of solids in protoplanetary disks. Perhaps, from such a model, we can read something about how sensitive the architecture of the resultant planetary system is to the initial conditions, such as M_{disk} and J_{disk} , as well as on the assumed microphysics, such as α and coagulation sticking coefficient. The model relies on two dominant and interdependent physical processes, aerodynamic forces, which make the radial transport of solid particles possible and coagulation, which makes the emergence of large bodies like planetesimals possible. The interplay of time scales characterizing these processes produces the final radial mass distribution of solids. In this initial paper we focus on the aerodynamic forces. We have calculated space-time distributions of radial and transverse velocities of the various-sized solid particles relative to the accreting gas. We have also calculated the global evolution of a single-sized, noncoagulating particles for a number of particle sizes. The case of unisized particles illustrates the differences in time evolution between the gas and the solids. Using our results we are able to put some limits on coagulation time scales, based on the premise that the evolution of solid material must engender planets.

In Sect. 2 we describe the evolution of the gaseous component of the disk. The methods used to calculate the effects of aerodynamical forces on solid particles are given in Sect. 3. In addition, Sect. 3 contains the results of specific calculations aimed at obtaining space-time distributions of radial and transverse velocities of solid particles. The methods and results of solid material evolution calculations are presented in Sect. 4. Finally, in Sect. 5 we summarize our findings and discuss some of the implications of our results.

2. The evolution of the gas

The evolution of the gas in a viscous protoplanetary disk is determined from the axisymmetric equations of continuity and motion. Cylindrical polar coordinates (r, ϕ, z) are used, with $z = 0$ corresponding to a disk midplane (equator). Because the disk is explicitly assumed to be turbulent, quantities such as gas density and velocity are broken up into mean and fluctuating parts:

$$\rho = \bar{\rho} + \rho' \quad \text{and} \quad \mathbf{V} = \bar{\mathbf{V}} + \mathbf{V}' \quad (1)$$

The equations are expanded out and the Reynolds averaging technique is applied to obtain equations describing the large-scale, mean behavior of the gas. The general forms of the mean equations for an axisymmetric disk with negligible *molecular* viscosity are given by Cuzzi et al. (1993). The effects of turbulence manifest themselves by the presence of correlation terms, $\overline{V'_i V'_j}$, $\overline{\rho' V'_i}$, and $\overline{\rho' V'_i V'_j}$ in the large-scale equations. The presuming that $\rho' \ll \bar{\rho}$ makes it possible to neglect the triple correlations $\overline{\rho' V'_i V'_j}$. The gas velocity correlations are

expressed in terms of *turbulent* viscosity $\nu = (1/3)\alpha C_s H$, turbulent velocity $V_t = \sqrt{\alpha} C_s$, and gradients of the mean velocity: $\overline{V'_i V'_i} = V_t^2/3$ and $\overline{V'_i V'_j} = -\nu(\partial \bar{V}_i / \partial x_j + \partial \bar{V}_j / \partial x_i)$. In expressing ν and V_t in terms of the gas speed of sound C_s and disk half-thickness H we use the standard α -disk model and assume that the Rossby number is of the order of unity. The correlations of the form $\overline{\rho' V'_i}$ are modeled by the gradient diffusion hypothesis: $\overline{\rho' V'_i} = -D \nabla \bar{\rho}$, with D being the coefficient of turbulent diffusivity. Canuto & Battaglia (1988) argued that $D = \nu \text{Ko}^3$, where $\text{Ko} = 1.2 - 1.7$ is the Kolmogorov constant.

As we are concerned here with the evolution of the radial distribution of the gas, we assume $\bar{V}_z = 0$ and ignore the vertical dependence of physical quantities describing the state of the disk. Under such assumptions the only nonvanishing correlations are:

$$\overline{V_r'^2} = \overline{V_\phi'^2} = \overline{V_z'^2} = \frac{1}{3} V_t^2 \quad (2)$$

$$\overline{V_r' V_\phi'} = -\nu r \frac{\partial}{\partial r} \left(\frac{\bar{V}_\phi}{r} \right) \quad (3)$$

$$\overline{\rho' V_r'} = -D \frac{\partial \bar{\rho}}{\partial r} \quad (4)$$

The r component of the equation of motion determines the large-scale tangential velocity. We anticipate that a protoplanetary disk is geometrically thin. In a thin accretion disk the large-scale velocities are such that $\bar{V}_\phi \gg \bar{V}_r \sim \nu/r$ and the r component of the equation of motion reduces to:

$$\begin{aligned} \frac{\overline{V_\phi'^2}}{r} &= \frac{V_k^2}{r} + \frac{1}{\bar{\rho}} \frac{\partial \bar{P}}{\partial r} + \frac{1}{\bar{\rho}} \frac{\partial}{\partial r} \left(\frac{\bar{\rho} V_t^2}{3} \right) \\ &\quad - \frac{2D}{\bar{\rho}} \frac{\partial \bar{\rho}}{\partial r} \frac{\partial \bar{V}_r}{\partial r} - \frac{\bar{V}_r}{\bar{\rho} r} \frac{\partial}{\partial r} \left(r D \frac{\partial \bar{\rho}}{\partial r} \right) \end{aligned} \quad (5)$$

Here $V_k = (GM/r)^{1/2}$ is the Keplerian velocity and M is the mass of the central star. Of the five terms on the right-hand side of Eq. (5) the first, due to centrifugal acceleration, is the largest. The second, due to the gas pressure gradient, is smaller by a factor of the order of $(H/r)^2$. The third, "turbulent pressure" term, is smaller by a factor of the order of $(V_t/C_s)^2 (H/r)^2$. The two last terms, due to turbulent diffusion, are smaller by a factor of the order of $\alpha (H/r)^2 (\bar{V}_r/V_k)$. Thus the existence of sub-sonic turbulence does not influence the mean tangential velocity of the gas, which is slightly smaller than the Keplerian velocity because $\partial \bar{P} / \partial r < 0$. This small difference is crucial for the gas-solid interaction, but unimportant for the evolution of the gas, where $\bar{V}_\phi = V_k$ approximation is sufficient.

The mean radial velocity of the gas is computed from the r component of the equation of motion. At the lowest order, this component can be written as

$$\bar{\rho} \bar{V}_r - D \frac{\partial \bar{\rho}}{\partial r} = -3r^{-1/2} \frac{\partial}{\partial r} \left(r^{1/2} \bar{\rho} \nu \right) \quad (6)$$

The convective mass flux based on an average radial velocity (the first term on the left-hand side of Eq. (6)) is, in general, of the

same order of magnitude as the diffusive mass flux (the second term on the left-hand side of Eq. (6).) Together, they transport as much mass as the conservation of angular momentum allows (the right-hand side of Eq. (6)).

The Reynolds averaged continuity equation in the absence of sources is

$$\begin{aligned}\frac{\partial \bar{\rho}}{\partial t} &= -\frac{1}{r} \frac{\partial}{\partial r} (r \bar{\rho} \bar{V}_r + r \bar{\rho}' \bar{V}_r') \\ &= -\frac{1}{r} \frac{\partial}{\partial r} \left(r \bar{\rho} \bar{V}_r - r D \frac{\partial \bar{\rho}}{\partial r} \right)\end{aligned}\quad (7)$$

Substituting \bar{V}_r from Eq. (6) into Eq. (7) and integrating over the z coordinate we obtain the familiar equation for time evolution of the surface density ($\Sigma = \int \bar{\rho} dz$) of the gas

$$\frac{\partial \Sigma}{\partial t} = \frac{3}{r} \frac{\partial}{\partial r} \left(r^{1/2} \frac{\partial}{\partial r} \left[\nu \Sigma r^{1/2} \right] \right)\quad (8)$$

Note that Eq. (8) does not depend on turbulent diffusivity, as it only encapsulates conservation of mass and angular momentum. Because turbulent viscosity, ν , is not an explicit function of time, but instead depends only on the *local* conditions within a disk, ν can be expressed as $\nu = \nu(\Sigma, r)$ and Eq. (8) can be solved subject to boundary conditions on the inner and outer edges of a disk and the opacity law. Given $\Sigma(r, t)$, we can algebraically find all other disk variables. In particular, \bar{V}_r can be calculated from Eq. (6). Beware that the average radial velocity based on Reynolds averaging *does not* give an accretion rate, or $-2\pi r \Sigma \bar{V}_r \neq \dot{M}$. Instead, the sum of convective and diffusive fluxes give the proper accretion rate, $\dot{M} = -2\pi r \Sigma \bar{V}_r + 2\pi r D (\partial \Sigma / \partial r)$.

The methods of how to solve Eq. (8) and how to calculate other physical quantities describing the state of the protoplanetary disk are given in papers by Ruden & Pollack (1991) and Reyes-Ruiz & Stepinski (1995). Here we follow the methodology of Reyes-Ruiz & Stepinski³. In our numerical calculations, we start from the initial surface density profile of the form

$$\Sigma(t=0, r) = \Sigma_0 [1 + (r/r_0)^2]^{-s}\quad (9)$$

This distribution corresponds to Σ being practically uniform between the inner radius, which we have chosen to be $r_{in} = 0.037$ AU, and r_0 . The particular choice of r_{in} is not important as long as it is much smaller than the size of the disk. Values of r_0 , Σ_0 , and s are calculated to correspond to the desired initial disk mass and its angular momentum. For calculations presented in this paper we started with a disk of $0.245 M_\odot$ and an angular momentum of 5.6×10^{52} g cm² s⁻¹. These correspond to an initial surface density distribution characterized by $\Sigma_0 = 10^4$ g cm⁻² and $r_0 = 15$ AU, initial conditions that correspond closely to those considered "standard" in protoplanetary disk evolution calculations (Ruden & Pollack 1991). We examine disk evolution for two values of α : $\alpha = 0.01$ and $\alpha = 0.001$.

³ Reyes-Ruiz & Stepinski include the magnetic field in their considerations. Here we are using their numerical code but we explicitly exclude magnetic fields.

The evolution of a gaseous disk proceeds according to well established principles: the surface density decreases as the mass is lost to the central star (see Figs. 4 and 5), the temperature decreases as well, and the disk spreads as a certain portion of the disk's mass moves outward, carrying angular momentum. The physical quantities describing the state of the gas change dramatically during the evolution, thus constantly changing the aerodynamic regime encountered by solid particles suspended in the gas.

3. Aerodynamic forces on solid particles

The aerodynamics of solid bodies in the context of the solar nebula was first studied by Weidenschilling (1977). However, whereas his work pertained to a quiescent gas environment, we consider the aerodynamics of solids particles in a turbulent disk. The presence of turbulence complicates the problem because of: a) the existence of the mean radial velocity of the gas, b) the diffusion of solids due to collective action of turbulent eddies advecting particles in all directions. In accordance with the principles outlined in Sect. 1, we not only consider a turbulent disk, but we calculate the space-time variations of gas conditions in a self-consistent manner. We want to investigate the global evolution of solid bodies with sizes from $\sim \mu\text{m}$ to few hundreds of meters embedded in the accreting turbulent gas. The basic time evolution equation for a "fluid" of solid particles of mass m is given by

$$\begin{aligned}\rho_d \frac{d\mathbf{V}_d}{dt} &= -\rho_d \nabla \Psi - \rho_d \frac{\mathbf{V}_d - \mathbf{V}}{t_s(m)} \\ &= -\rho_d \nabla \Psi - \rho_d \frac{\mathbf{v}}{t_s(m)}\end{aligned}\quad (10)$$

where Ψ is the gravitational potential, \mathbf{v} is the relative velocity between a particle and the gas, and t_s is the so-called stopping time defined as $t_s(m) = mv/F_D$. Here $v = |\mathbf{v}| = \sqrt{v_r^2 + v_\phi^2}$, and F_D is the drag force, which depends on the size of the particle, the density of the gas, and the speed of the particle relative to the gas. Subscript d denotes quantities describing the state of the solids⁴, whereas quantities describing the gas have no subscript. We now proceed in a fashion similar to that described in Sect. 2 for the gas. Particles density and velocity are divided into mean and fluctuating parts:

$$\rho_d = \bar{\rho}_d + \rho'_d \quad \text{and} \quad \mathbf{V}_d = \bar{\mathbf{V}}_d + \mathbf{V}'_d\quad (11)$$

Radial and tangential components of Eq. (10) are expanded out as we seek to calculate \bar{V}_{rd} and $\bar{V}_{\phi d}$. We follow Cuzzi et al. (1993) in expressing correlation terms $\overline{V'_{id} V'_{jd}}$ as $\overline{V'_i V'_j} / \text{Sc}$, where Sc is called the Schmidt number and is given by the expression

$$\text{Sc} = (1 + \Omega_k t_s) \sqrt{1 + \frac{\bar{v}^2}{V_1^2}}\quad (12)$$

⁴ In this paper solid particles are called particles, solids, dust, or grains interchangeably. We have chosen subscript d for "dust" to denote all quantities describing solid particles.

Table 1. Summary of drag laws used in our calculations.

Reynolds number $Re = 2s\rho v/\eta$	Stokes law $\lambda < 4s/9$	Epstein law $\lambda > 4s/9$
$Re < 1$	$F_D = 24Re^{-1}F$	$F_D = \frac{4\pi}{3}\rho s^2 v C_s$
$1 < Re < 800$	$F_D = 24Re^{-0.6}F$	
$Re > 800$	$F_D = 0.44F$	
	$F = \pi s^2 \rho \frac{v^2}{2}$	

Here Ω_k denotes the Keplerian angular velocity, and the turnover time of turbulence is approximately given by $1/\Omega_k$ as we have assumed that the Rossby number is of the order of unity. Particles are imperfectly coupled to turbulent eddies because: a) the lifetime of an eddy can be shorter than the stopping time of a particle (this is described by the first factor on the right-hand side of Eq. (12)), b) a particle has a systematic relative velocity with respect to the gas and can cross an eddy in time shorter than the stopping time (this is described by the second factor on the right-hand side of Eq. (12)). The correlations $\overline{\rho'_d V'_d}$ are expressed as $-D_d \nabla \overline{\rho_d}$ and the diffusion coefficient is given by $D_d = D/Sc$ (see Cuzzi et al. 1993, as well as Dubrulle et al. 1995).

Taking advantage of the fact that $\overline{V_{rd}} \ll C_s$ we can write the r component of Reynolds averaged Eq. (10) as

$$\frac{\overline{V_{\phi d}^2}}{r} = \frac{V_k^2}{r} + \frac{1}{\overline{\rho_d}} \frac{\partial}{\partial r} \left(\frac{\overline{\rho_d} V_t^2}{3Sc} \right) + \frac{\overline{v_r}}{t_{s**}} - \frac{2D}{\overline{\rho_d} Sc} \frac{\partial \overline{\rho_d}}{\partial r} \frac{\partial \overline{V_{rd}}}{\partial r} - \frac{\overline{V_{rd}}}{\overline{\rho_d} r} \frac{\partial}{\partial r} \left(\frac{rD}{Sc} \frac{\partial \overline{\rho_d}}{\partial r} \right) \quad (13)$$

When averaging the gas-solids coupling term we assume that $\overline{\rho_d v}/t_s = \overline{\rho_d} \overline{v}/t_{s**}$, where $t_{s**} = t_s(v)$ if $v > V_t$ and $t_{s**} = t_s(V_t)$ if $v < V_t$. In addition, we have assumed that $\overline{\rho'_d V'_{rd}} - \overline{\rho'_d} \overline{V'_{rd}} \approx 0$. Of the five terms on the right-hand side of Eq. (13), the first is the largest. The second, fourth, and fifth terms, all due to coupling of particles to turbulent eddies, are negligible for subsonic turbulence. Thus, $\overline{V_{\phi d}}$ differs slightly from V_k because of $\overline{v_r}/t_{s**}$ term.

Averaging the ϕ -component of Eq. (10) we can calculate the mean radial velocity of particles. Using the fact that $\overline{V_{\phi d}} \approx V_k$ we obtain at the lowest order

$$\overline{\rho_d} \overline{V_{rd}} - \frac{D}{Sc} \frac{\partial \overline{\rho_d}}{\partial r} = -3r^{-1/2} \frac{\partial}{\partial r} \left(r^{1/2} \overline{\rho_d} \frac{\nu}{Sc} \right) - \frac{2\overline{\rho_d} \overline{v_\phi}}{\Omega_k t_{s**}} \quad (14)$$

Note the formal similarity between Eqs. (13)-(14), describing the motion of particles, and Eqs. (5)-(6), describing the motion of the gas. Due to the coupling of particles to turbulent eddies of the gas, they experience “pressure” (the second term on the right-hand side of Eq. (13)), as well as “viscosity” (the first term on the right-hand side of Eq. (14)). In addition there are differences between mean velocities of particles and the gas resulting in the drag force (terms proportional to \overline{v} in Eqs. (13)-(14)).

3.1. Drag laws

To close the system of Eqs. (13) and (14) we need to specify $t_s(m, v, \text{gas}) = mv/F_D$. We assume that a solid particle is a sphere of radius s and bulk density ρ_s , thus $s = (3m/4\pi\rho_s)^{1/3}$. The drag regime depends on the size of the mean free path of gas molecules, λ , as compared with s . Table 1 shows the forms of different drag laws used in our calculations. The gas molecular viscosity η is given by the formula $\eta = \rho\lambda C_s/2$, so the Reynolds number can be expressed as $Re = 4(v/C_s)(s/\lambda)$. As we do not expect that particles have supersonic velocities with respect to the gas, the Epstein regime is tantamount to $Re < 1$. In the $Re < 1$ regime the transition from Stokes law to Epstein law occurs for $\lambda/s = 4/9$. We calculated the mean free path of gas molecules from the usual formula $\lambda = 1/n\sigma_0$, where n is the number density of gas molecules and σ_0 is the total scattering cross section. The major constituent of the gas in protoplanetary disks is molecular hydrogen. Taking the geometrical approximation to the cross section we obtain $\lambda = m_{H_2}/\pi\rho r^2_{H_2}$. Because the state of the gas is known (see Sect. 2) the mean free path can be calculated at any time and for any disk location. This information combined with the data on particle mass and relative speed (or V_t if $v < V_t$) sets the value of the Reynolds number and the drag regime, thus allowing the closure of the system of Eqs. (13) and (14), albeit in the implicit form, as knowledge of a particle’s relative speed is required to establish a drag regime. This implicitness of our equations is not a serious problem inasmuch as the solution is obtained numerically anyhow and an appropriate algorithm is applied to achieve the self-consistency of the solution.

3.2. Space-time distribution of solid particles mean velocities

Eqs. (13) and (14) constitute the closed system for two unknowns, $\overline{v_r}$ and $\overline{v_\phi}$, because $\overline{V_{\phi d}}$ can be eliminated using the relation $\overline{V_{\phi d}} = \overline{v_\phi} + \overline{V_\phi}$ with $\overline{V_\phi} = V_k + (r/2\overline{\rho} V_k)(\partial \overline{\rho}/\partial r)$ and $\overline{V_{rd}}$ can be eliminated using the relation $\overline{V_{rd}} = \overline{v_r} + \overline{V_r}$ given by Eq. (6). With such an elimination, and keeping only terms linear in $\overline{v_r}$ and $\overline{v_\phi}$, we obtain

$$2\overline{v_\phi} - \frac{\overline{v_r}}{\Omega_k t_{s**}} = -\frac{1}{\overline{\rho}} \frac{\partial \overline{P}}{\partial r} \frac{1}{\Omega_k} \quad (15)$$

and

$$\overline{v_r} + \frac{2\overline{v_\phi}}{\Omega_k t_{s**}} = -\overline{V_r} - 3r^{-1/2} \frac{\partial}{\partial r} \left(r^{1/2} \frac{\nu}{Sc} \right) + \frac{(D-3\nu)}{Sc} \frac{1}{\overline{\rho_d}} \frac{\partial \overline{\rho_d}}{\partial r} \quad (16)$$

The time evolution of $\overline{v_r}$ and $\overline{v_\phi}$ can be found for particles of any given size by solving the system of Eqs. (15)–(16) as all coefficients in these equations depend on properties of the gas and thus are known functions of space and time. The last term in Eq. (16) is the exception as it depends on the density of the particles. The space-time evolution of particles density is discussed in Sect. 4, here we remark that calculating particle densities requires the knowledge of $\overline{v_r}$ and $\overline{v_\phi}$. Therefore, it

general, Eqs. (15–16) have to be solved *simultaneously* with the particles density evolution Eq. (18). Note, however, that the last term in Eq. (16) vanishes if $D = 3\nu$, which is consistent with estimation of D by Canuto & Battaglia (1988) (see the beginning of Sect. 2). In the bulk of our calculations presented in this paper we assume $D = 3\nu$. This permits the discussion of particles mean velocities independently from the discussion of their densities. We have also performed calculations for $D = \nu$, which requires the solution of a coupled velocity-density problem, and have found only expected, quantitative differences between the results for $D = \nu$ and the results for $D = 3\nu$. Thus, it seems that although the condition $D = 3\nu$ is computationally advantageous, there is nothing physically unique about it.

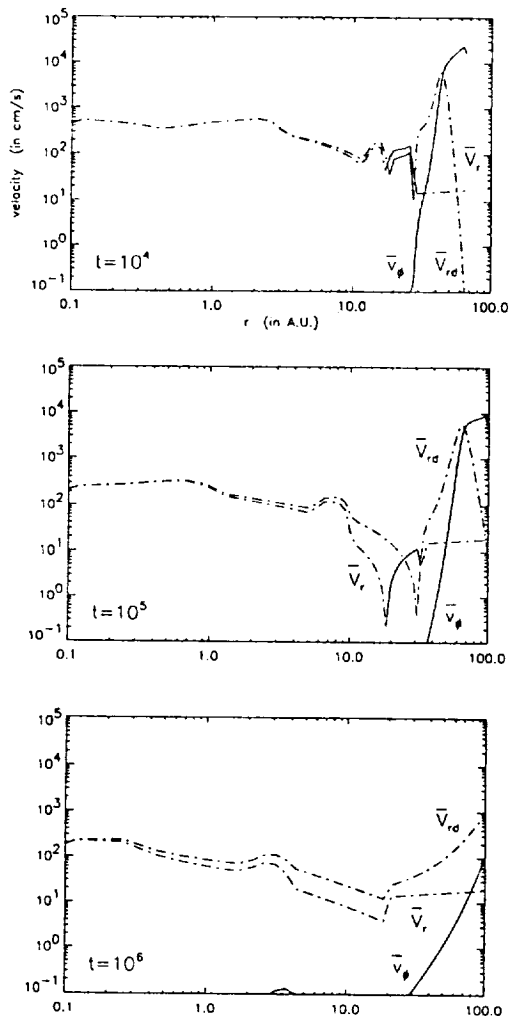


Fig. 1. Radial distributions of \overline{V}_{rd} , the mean radial velocity of a solid particles; \overline{V}_r , the mean radial velocity of the gas; and \overline{v}_ϕ , the mean *relative* transverse velocity between particles and the gas, respectively. The times shown are $t = 10^4$ yr, $t = 10^5$ yr, and $t = 10^6$ yr. Particle have all the same radius $s = 0.1$ cm. Solid lines indicate a positive velocity (an outward movement for radial velocities and particles faster then the gas for \overline{v}_ϕ), whereas dash-dotted lines indicate a negative velocity.

Let's consider the gas evolution scenario described in Sect. 2, which starts at $t = 0$ with a disk of $0.245 M_\odot$ and an angular momentum of $5.6 \times 10^{52} \text{ g cm}^2 \text{ s}^{-1}$. The evolution proceeds with dimensionless coefficient of viscosity $\alpha = 0.01$. Our goal is to calculate the time evolution of \overline{V}_{rd} and \overline{v}_ϕ for particles of different sizes embedded in an evolving gaseous disk. The knowledge of particle mean velocities is important inasmuch as these velocities capture the bulk of particle dynamics. Beware, however, that the contribution of turbulent diffusion to particles dynamics is crucial for explanation of certain features of their evolution. First, we have found out that very small particles, with $s < 0.1$ cm, can be considered perfectly coupled to the gas. Their mean velocities match the mean velocity field of the gas. On the other hand, very large particles, with $s \geq 10^5$ cm, can be considered completely decoupled from the gas. Their mean velocities remain practically unchanged with time. Particles with sizes between these two extremes are partially coupled to the gas.

Fig. 1 shows time evolution of \overline{V}_r (mean radial velocity of the gas), \overline{V}_{rd} (mean radial velocity of a particle), and \overline{v}_ϕ (tangential component of mean *relative* velocity between a particle and the gas) for particles with $s = 0.1$ cm. For the purpose of the present discussion we label such particles “small.” The tangential velocity of the gas is not shown in Fig. 1 as it always stays very close to the Keplerian velocity. As we have already mentioned in Sect. 2, \overline{V}_r is not always the accurate indicator of the mass flux. The distinctive feature of the mass flux distribution in the gaseous accretion disk is the existence of a stagnation radius that separates the region of gas accretion from the region of gas decretion. This stagnation radius moves outward during disk evolution. Examining Fig. 1 we notice that although \overline{V}_r has the same sense as the mass flux throughout the entire accretion zone and in the inner decretion zone, it is oriented inward in the outer decretion zone even so the mass flows outward there. This is because the transport of mass in the outermost disk, where the steep gradient of density is maintained, is dominated by turbulent diffusion. Inward convective mass flux is necessary to reduce the outward diffusive mass flux so that Eq. (6) is satisfied.

Small particles remain rather strongly coupled to the mean flow of the gas; \overline{v}_ϕ is very small and $\overline{V}_{rd} \approx \overline{V}_r$. Throughout the accreting part of the disk the magnitude of \overline{v}_ϕ remains within the same order of magnitude, about 10^{-3} cm/s at $t = 10^4$ yr, 10^{-2} cm/s at $t = 10^5$ yr, and finally 10^{-1} cm/s at $t = 10^6$ yr. In comparison, the Keplerian velocity in this region of the disk is in the range of 10^6 – 10^7 cm/s. The particles have super-gas (faster than the gas) mean tangential velocities and thus experience, on average, a tangential head wind. The particles have small super-gas mean radial velocities ($\overline{V}_{rd} < \overline{V}_r < 0$) and thus experience, on average, a radial head wind as well. Throughout the outer, decreting part of the disk, the particles are less coupled to the mean flow of the gas. The magnitude of \overline{v}_ϕ changes by orders of magnitude and can be as large as 10^4 cm/s at the outer edge of the disk. For times up to few $\times 10^4$ yr, the particles in the inner part of the gas decretion zone move on average outward with slightly sub-gas velocities, thus experiencing a radial tail

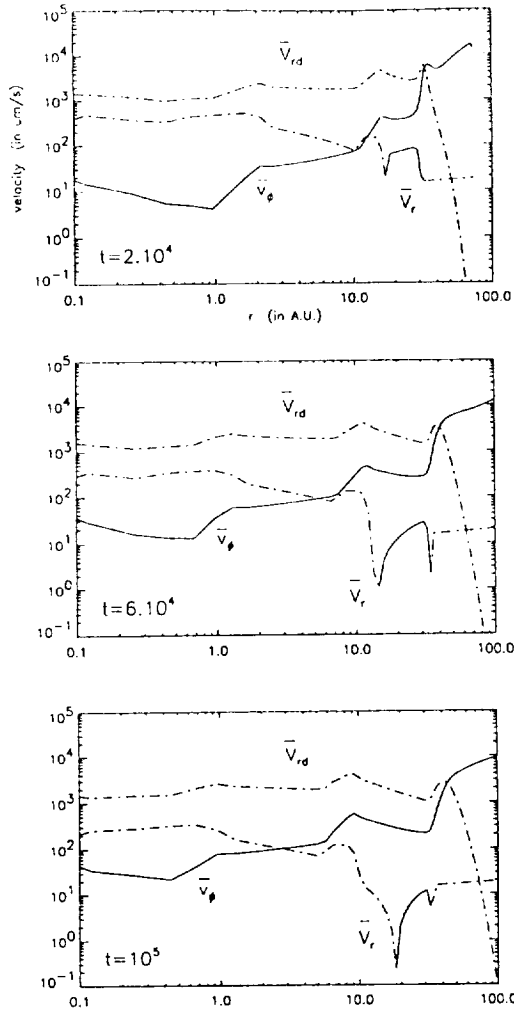


Fig. 2. Radial distributions of $\overline{V_{rd}}$, $\overline{V_r}$, and $\overline{v_\phi}$, respectively. The times shown are $t = 2 \times 10^4$ yr, $t = 6 \times 10^4$ yr, and $t = 10^5$ yr. Particles have a radius $s = 10$ cm. Solid lines indicate a positive velocity (an outward movement for radial velocities and particles faster than the gas for $\overline{v_\phi}$), whereas dash-dotted lines indicate a negative velocity.

wind. However, in the outer part of the gas accretion zone, the average radial velocity of small particles is directed inward, as is the average radial velocity of the gas. Nevertheless, mass fluxes of both particles and the gas are outward, as they are dominated by turbulent transport.

Fig. 2 shows time evolution of $\overline{V_r}$, $\overline{V_{rd}}$, and $\overline{v_\phi}$ for particles with $s = 10$ cm. We label such particles “medium.” Medium particles are much less coupled to the mean flow of the gas than small particles: $\overline{v_\phi}$ for medium particles is orders of magnitude larger than $\overline{v_\phi}$ for small particles. There is not much change in the magnitude of $\overline{v_\phi}$ throughout the disk evolution. Medium particles move on average with super-gas tangential velocities everywhere in a disk and any time during the disk evolution. Also, medium particles always move on average inward. Note that $|\overline{V_{rd}}| \gg |\overline{V_r}|$, thus these particles are “fast” in their ra-

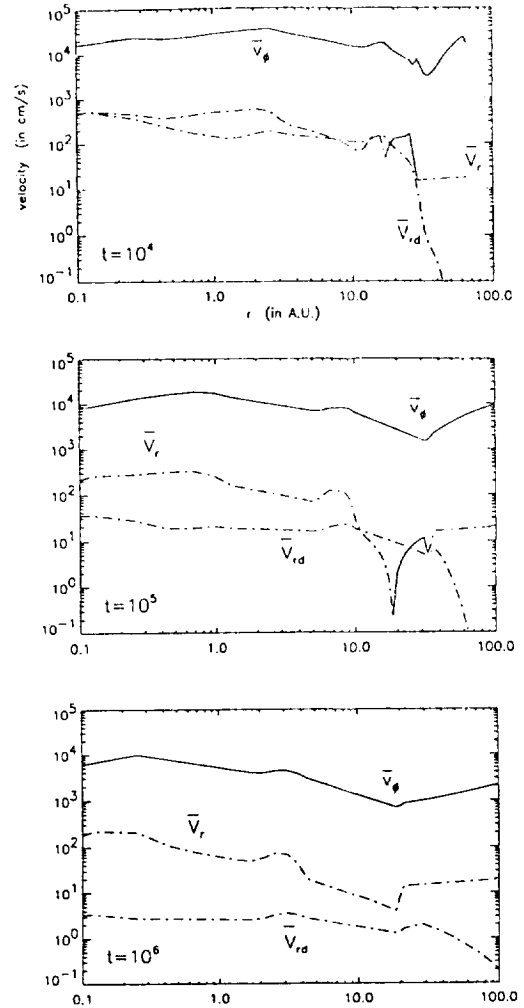


Fig. 3. Radial distributions of $\overline{V_{rd}}$, $\overline{V_r}$, and $\overline{v_\phi}$, respectively. The times shown are $t = 10^4$ yr, $t = 10^5$ yr, and $t = 10^6$ yr. Particles have a radius $s = 10^4$ cm. Solid lines indicate a positive velocity (an outward movement for radial velocities and a particle faster than the gas for $\overline{v_\phi}$), whereas dash-dotted lines indicate a negative velocity.

dial movement. With average radial velocities of the order of 10^3 – 10^4 cm/s, medium particles have evolutionary time scales comparable to 10^4 yr. Therefore, handling of the medium particles encounters the problem described in Sect. 1. As their evolutionary time scale is comparable to the time the gaseous disk needs to forget the arbitrary initial conditions, their properties at later times may be sensitive to the initial conditions. To circumvent this problem we introduce medium particles into the gas at $t = 10^4$ yr, instead of $t = 0$ as we have done for the small particles. Also, we finish our calculations for medium particles at $t = 10^5$ yr, as medium particles are severely depleted after this time. In fact, there would be no medium particles left in the disk after this time if not for the contribution of turbulent diffusion to the dynamics of particles.

Fig. 3 shows time evolution of \overline{V}_r , \overline{V}_{rd} , and \overline{v}_ϕ for particles with $s = 10^4$ cm. We label such particles “large.” Large particles are only weakly coupled to the mean gas flow: \overline{v}_ϕ remains relatively large as particles move with almost a Keplerian velocity, faster than the gas that is pressure supported. Large particles, much like the medium particles, move with super-gas tangential velocities everywhere in a disk and at any time during the disk evolution. They also always move inward. Note, however, that conversely to the case of the medium particles, for $t \geq 10^5$ yr, $|\overline{V}_{rd}| \ll |\overline{V}_r|$, so the radial movement of large particles is insignificant, and becomes more insignificant with time. Thus, large particles are “slow” in their radial movement. They remain on Keplerian orbits drifting very slowly inward.

4. Global evolution of single-sized, noncoagulating particles

In order to visualize the global effects of solid particles decoupling from the gas, it is convenient to calculate the evolution of single-sized, noncoagulating particles. This is a hypothetical evolutionary scenario, by itself not likely to be pertinent to establishing the architecture of an emerging planetary system. Nevertheless, it illustrates the difference in time evolution between the gas and the solids. It provides a valuable point of reference for more realistic calculations. In the case of $D \neq 3\nu$, computation of space-time distribution of $\overline{\rho}_d$ is necessary to establish a particle velocity field (see Sect. 3.2.) Here, however, we assume that $D = 3\nu$ and velocity of particles are known beforehand.

The ensemble of identical particles can be treated within the framework of hydrodynamics, or as a “fluid” with “pressure” and “viscosity” provided by coupling between particles and turbulent eddies of the gas. By analogy with the gas, the evolution equation can be obtained from mass conservation supplemented by the ϕ component of the equation of motion. The Reynolds averaged continuity equation for fluid of single-sized particles in the absence of sources is

$$\begin{aligned} \frac{\partial \overline{\rho}_d}{\partial t} &= -\frac{1}{r} \frac{\partial}{\partial r} \left(r \overline{\rho}_d \overline{V}_{rd} + r \overline{\rho}'_d \overline{V}'_{rd} \right) \\ &= -\frac{1}{r} \frac{\partial}{\partial r} \left(r \overline{\rho}_d \overline{V}_{rd} - r \frac{D}{Sc} \frac{\partial \overline{\rho}_d}{\partial r} \right) \end{aligned} \quad (17)$$

Substituting \overline{V}_{rd} from Eq. (14) into Eq. (17) and integrating over the z coordinate we obtain the equation for time evolution of Σ_d , the surface density of solid particles

$$\begin{aligned} \frac{\partial \Sigma_d}{\partial t} &= \frac{3}{r} \frac{\partial}{\partial r} \left(r^{1/2} \frac{\partial}{\partial r} \left[\frac{\nu}{Sc} \Sigma_d r^{1/2} \right] \right) \\ &\quad + \frac{1}{r} \frac{\partial}{\partial r} \left(\frac{2r \Sigma_d \overline{v}_\phi}{\Omega_k t_{s*}} \right) \end{aligned} \quad (18)$$

One can also define \dot{M}_d as the accretion rate of a solid material through a disk. As in the case of the gas, the mass flux of solid particles is the sum of convective and diffusive fluxes. Unlike Eq. (8), which directs the evolution of the gas, Eq. (18) is not a diffusive-type equation. Instead, it is an advection-diffusion equation. Because Eqs. (8) and (18) are of different types, a

single numerical method that would concurrently advance both of them in time is difficult to contrive. Taking advantage of our assumption that the evolution of the gas is not affected by the presence of solid particles, we first solve Eq. (8) using an implicit scheme, then obtain the space-time distribution of \overline{v}_ϕ by methods described in Sect. 3, and finally solve Eq. (18) using the operator splitting method. In such a method the advective term in (18) is treated by numerical method of characteristics, whereas an implicit scheme is applied to the diffusion term.

In general, particles can be divided into “long-lived” (LL), characterized by evolutionary time scales comparable to or longer than the evolutionary time scale of the gas, and “short lived” (SL), characterized by time scales shorter than the lifetime of the gaseous disk. The small particles, which are strongly coupled to the gas and thus evolve on an approximately viscous time scale, and large particles, which are decoupled from the gas and move toward the central star very slowly, are LL particles. The medium particles have radial velocities larger than the radial velocity of the gas, they accrete quickly onto the central star, and therefore are SL particles. The terms LL and SL refer to an *average* lifetime of a particle. Because of the existence of a random component in particle motion, few individual SL particles may survive for a long time, and some individual LL particles may have a short lifetime.

Fig. 4 shows an evolution of the surface density for LL particles. Our computation starts at $t = 0$ with a disk of $0.245 M_\odot$ and an angular momentum of $5.6 \times 10^{52} \text{ g cm}^2 \text{ s}^{-1}$. Evolutionary scenarios with $\alpha = 0.01$ and $\alpha = 0.001$ are calculated. The initial surface density of solid material is $\Sigma_d(r, t = 0) = 10^{-2} \Sigma(r, t = 0)$ to reflect that about 1% of disk mass is in the form of solid particles. We follow the evolution of LL particles up to $t = 10^6$ yr. Solids with a radius of $s = 0.1$ cm represent small particles, and solids with a radius of 10^4 cm represent large particles.

If the entire mass of the solid material is concentrated in particles smaller than 0.1 cm, then solids are perfectly coupled to the gas and the radial distribution of solids follows the radial distribution of the gas as indicated on Fig. 4 by dotted lines. For the purpose of the present discussion we refer to such a distribution of solids as the putative distribution (it differs from the distribution of gas by a factor of 100). Now assume, however, that the solid material is concentrated into 0.1 cm particles. It is clear from Fig. 4 that such solids slowly decouple from the gas. First, let’s discuss the $\alpha = 0.01$ scenario. At $t = 10^4$ yr the decoupling of small particles from the gas is not yet pronounced. The decoupling becomes noticeable at $t = 10^5$ yr, when solids located at the outer edge of the disk spread outward at the slower rate than the gas. This, combined with the fact that the inward radial velocity of solids is slightly larger than the radial velocity of the gas (see Fig. 1), causes the surface density of solids within the inner 10 AU to be enhanced with respect to the putative distribution. At $t = 10^6$ yr the difference between the surface density of small particles and putative surface density increases. Within the inner ~ 10 AU the mass density of particles is enhanced with respect to the putative density, but outward of ~ 10 AU the mass density of particles is actually

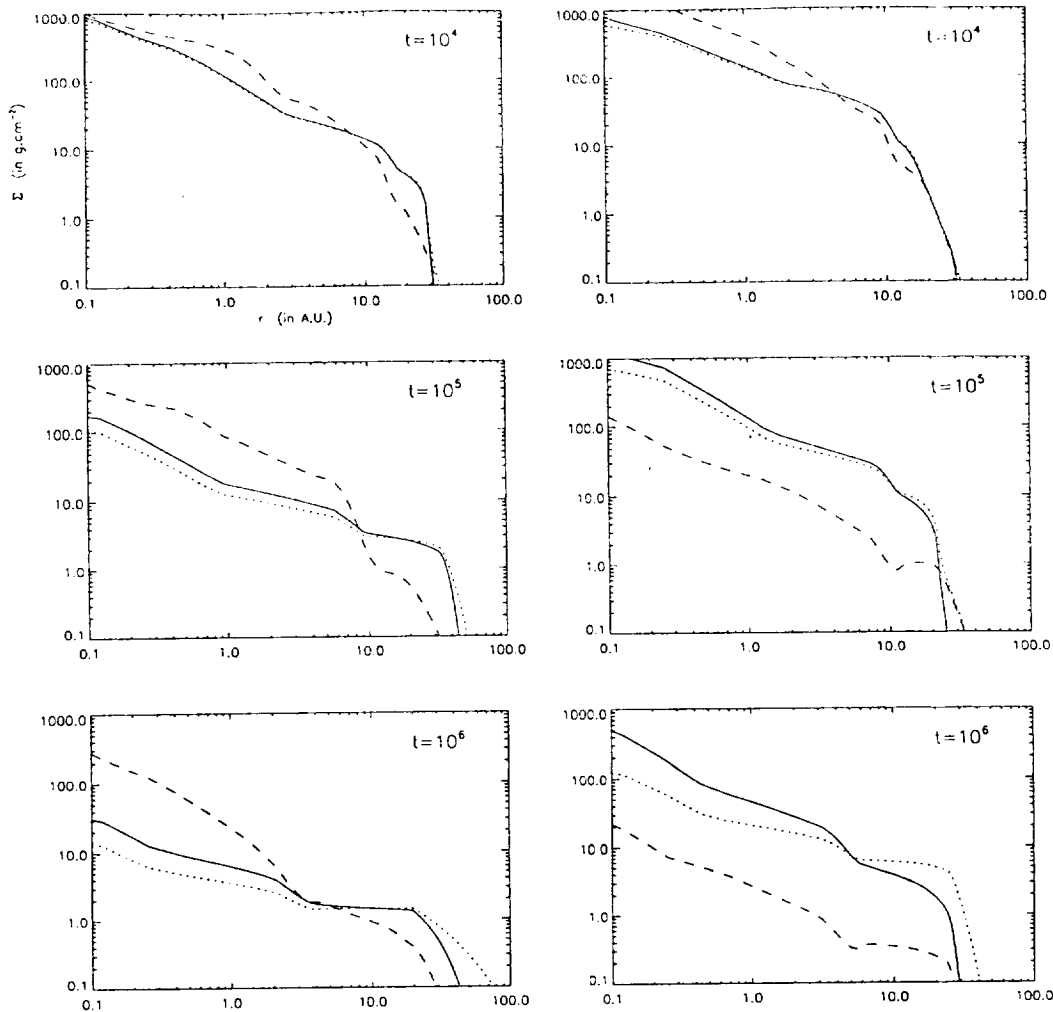


Fig. 4. Radial distributions of surface density of solids at selected times ($t = 10^4$ yr, $t = 10^5$ yr, and $t = 10^6$ yr) for LL particles. The left-hand panels correspond to the evolutionary scenario with $\alpha = 0.01$, whereas the right-hand panels correspond to the scenario with $\alpha = 0.001$. Dotted lines show the surface density of the gas $\times 10^{-2}$. Solid lines show the surface density of 0.1 cm particles and dashed lines show the surface density of 10^4 cm particles.

depleted as compared to the putative density. The $\alpha = 0.001$ shows a similar behavior of small particles.

Now assume that the solid material is concentrated into 10^4 cm particles. Examination of Fig. 4 reveals that such large particles are largely decoupled from the gas. In the $\alpha = 0.01$ scenario the radial distribution of surface density of such particles in the inner disk shows relatively little change during $t = 10^6$ yr of evolution. Therefore, a large difference between the mass density of large particles and the putative mass density develops with time in the inner portion of the disk. In the outer portion of the disk large particles evolve faster than the putative mass density, again resulting in build up of a significant difference between both distributions with time. Overall the radial distribution of large particles steepens with time, whereas the putative mass distribution flattens. In the $\alpha = 0.001$ scenario, after some initial time, large particles evolve faster than the putative mass

distribution. This is because the $\alpha = 0.001$ disk evolves more slowly than the $\alpha = 0.01$ disk and its gas density remains high for much longer. That, in turn, makes the drag force on large particles stronger and longer lasting, thus enabling them to evolve faster. Again, a large difference between the mass density of large particles and the putative mass density develops with time.

Fig. 5 shows an evolution of the surface density for SL particles. Our gas computation starts at $t = 0$ with a disk of $0.24 M_{\odot}$ and an angular momentum of $5.6 \times 10^{52} \text{ g cm}^2 \text{ s}^{-1}$. Evolutionary scenarios with $\alpha = 0.01$ and $\alpha = 0.001$ are calculated. To eliminate the influence of arbitrary initial conditions on the evolution of SL particles, for which evolutionary time scales are comparable to 10^4 yr, we start our particle computation at $t = 10^4$ yr with $\Sigma_d(r, t = 10^4) = 10^{-2} \Sigma(r, t = 10^4)$ and we follow their evolution up to $t = 10^5$ yr. Solid particles with radii 1 cm, 10 cm, and 10^3 cm are all short-lived and their evolu-

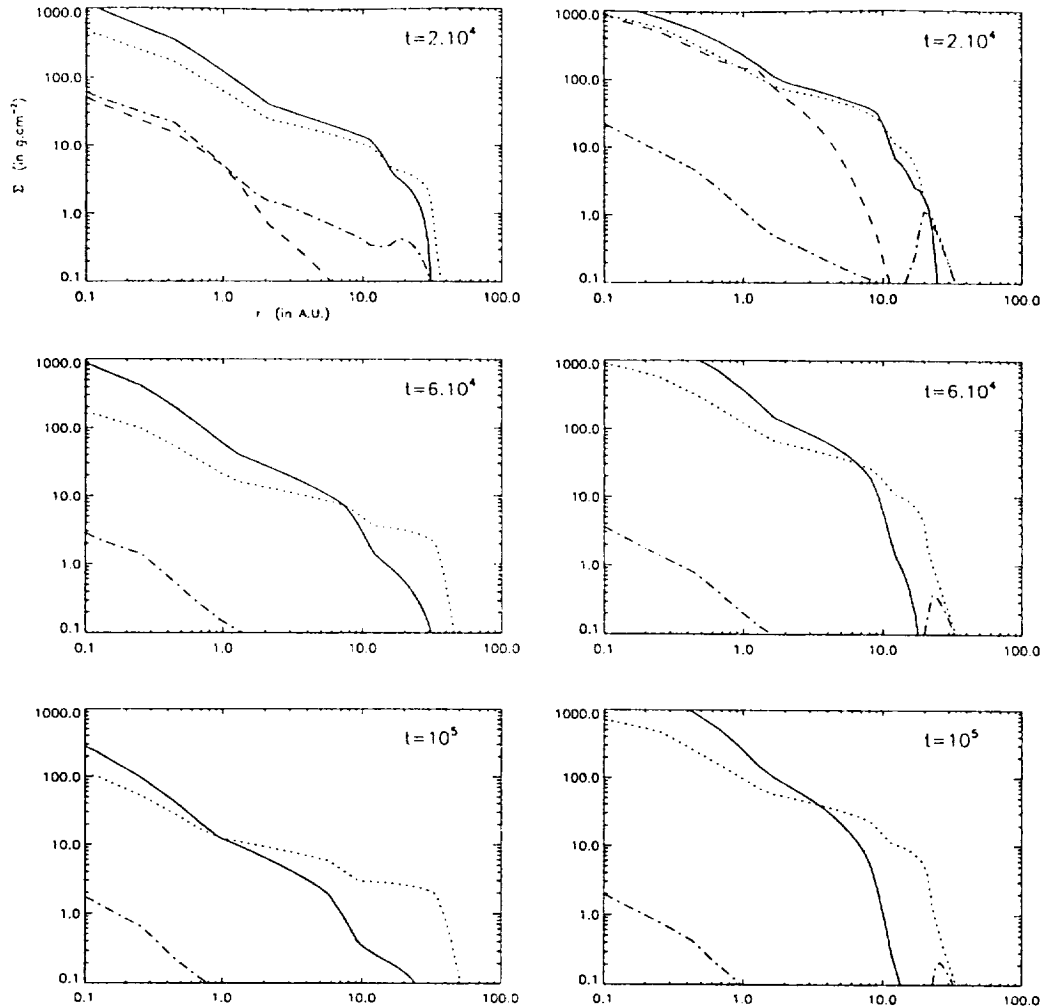


Fig. 5. Radial distributions of surface density of solids at selected times ($t = 2 \times 10^4$ yr, $t = 6 \times 10^4$ yr, and $t = 10^5$ yr) for SL particles. The left-hand panels correspond to the evolutionary scenario with $\alpha = 0.01$, whereas the right-hand panels correspond to the scenario with $\alpha = 0.001$. Dotted lines show the surface density of the gas $\times 10^{-2}$. Solid lines show the surface density of 1 cm particles, dashed lines show the surface density of 10 cm particles, and dash-dotted lines show the surface density of 10^3 cm particles.

tion is shown on Fig. 5. If solid material is concentrated in such particles, it decouples quickly from the gas and is lost to the central star in a relatively short period of time. The case of 10 cm particles offers the extreme example. Such particles are lost in less than a few $\times 10^4$ yr regardless of the magnitude of α . Solid material concentrated into 10^3 cm particles is lost in about 10^5 yr, whereas solids concentrated into 1 cm particles are all accreted in a few $\times 10^5$ yr. None of these SL particles survives in an average sense, until $t = 10^6$ yr. As can be seen from Fig. 5 radial distribution of the surface density for SL particles can be quite complicated. Consider, for example, 10^3 cm particles during the evolution characterized by $\alpha = 0.001$. Although most of them accrete quickly onto the central star, those initially located at the outer edge of the disk linger there for a relatively long time before starting their inward movement. This rather intricate be-

havior is the result of large radial and temporal changes in the aerodynamic regime encountered by particles.

5. Discussion

This paper represents an attempt to study the global evolution of solids in a viscously accreting protoplanetary disk. This is a first venture into a complex problem, and we have accordingly simplified the problem to mere essentials. Two central issues for modeling global evolution of solids are aerodynamic forces and coagulation processes. We have developed a numerical method to study the effects of aerodynamic forces. Adding a coagulation process to our numerical model will allow us to test whether the body of presently embraced theoretical concepts (outlined in Sect. 1), when applied all at once, leads to the formation of a planetary system that looks anything like our own. This will be

presented in the next paper. Despite the obvious limitation of studying aerodynamic forces alone, they yielded a number of interesting conclusions.

Perhaps the most interesting (and upon reflection the most obvious) result of our calculations is that solid particles that are larger than 0.1 cm are not really entrained in the gas. This finding can be best illustrated by following the total mass of solid particles in a disk as a function of time. Fig. 6 shows such a total mass evolution for particles of different sizes. Examination of Fig. 6 makes it clear that solids and gas evolve differently. This seems to preclude any cosmogonical theory that postulates that the radial distribution of solids remains in any particular relationship to the momentary radial distribution of the gas. In particular, our results suggest that the broadly used concept of the minimum mass solar nebula, in which the radial distribution of the gas in the disk is reconstructed from the radial distribution of the solid material as found in the present-day solar system, is conceptually flawed⁵. As our solar system is readily accessible to observation, it may seem quite salutary to use any data we have at hand to advance our knowledge about the progenitor solar nebula as well as other protoplanetary disks. However, our results show that such an approach, although intellectually appealing, is futile, as it must inevitably lead to spurious results. Instead of trying to *reconstruct* a protoplanetary disk from a planetary system, we should *simulate* the formation of a planetary system by means of comprehensive evolutionary calculations.

Weidenschilling (1988) discusses a variety of coagulation processes that are relevant for solar nebula conditions. Naturally, if a solar nebula exemplifies contemporaneously observable disks, these same processes are responsible for coagulation in all protoplanetary disks. For particles of the sizes considered here, the predominant mechanisms are coagulation due to radial motion, vertical settling, and turbulence. For our models of an accretion disk, characterized by a relatively small value of α , turbulent coagulation is generally slower than the coagulation due to the radial motion of particles. Vertical settling, which gives the fastest coagulation in the quiescent disk, is not very effective in the turbulent disk. Altogether, for the purpose of the present discussion, we may assume that coagulation is dominated by radial drift. The mass of the particle increases at the rate $dm/dt \approx \pi s^2 \bar{\rho}_d \Delta \bar{V}_r$, where $\Delta \bar{V}_r$ is assumed to be of the order of $|\bar{V}_{rd}|$. Thus, the characteristic coagulation time is $t_c = m/(dm/dt) \approx (\rho_s/\bar{\rho}_d)(s/\Delta \bar{V}_r)$. Using this formula, one can estimate a characteristic time scale of coagulation for various sized particles at different times and different disk locations. For example, consider a disk at $t = 10^5$ yr. Our model with $\alpha = 0.01$ gives $\bar{\rho}_d \sim 10^{-13}$ g cm⁻³ at 10 AU from the star for small and large particles, and $\bar{\rho}_d \sim 10^{-14}$ g for medium particles. Assuming ρ_s of about 1 g cm⁻³ and using Figs. 1–3 to estimate the value of $\Delta \bar{V}_r$, we calculate $t_c \approx 10^3$ yr for

small particles, $t_c \approx 10^4$ for medium particles and $t_c \approx 10^5$ yr for large particles (here we used $\Delta \bar{V}_\phi$ instead of $\Delta \bar{V}_r$ to estimate t_c , because $|\Delta \bar{V}_\phi| > |\Delta \bar{V}_r|$ for large particles). These estimations underscore the necessity of our global approach to the evolution of solid matter in a protoplanetary disk, especially for medium and large particles. The coagulation time scale for small particles is indeed short in comparison with their characteristic radial evolution time scale. A small particle moves only about 0.1 AU from its original location at 10 AU before it becomes a part of a larger particle. However, medium particles have coagulation time scales comparable to their radial evolution time scales. An average medium particle may travel all the way to the central star during its lifetime. This is also true for large particles, which take a long time to coagulate. A large particle has very slow radial velocity, but it can travel a long distance before coagulating into even bigger particle. Thus, a local approach may work for small particles that are slow and coagulate quite quickly. Medium particles coagulate quickly but are very fast, whereas large particles move slowly but they exist for a long time; in both cases global calculations are needed to calculate the radial distribution of solid matter.

Considering a turbulent instead of a quiescent disk is important for the physical conditions describing the gas and for aerodynamic forces and coagulation processes. The properties of the turbulent gaseous disk changes with time, thus changing aerodynamic regime encountered by particles. Even if coagulation of small particles happens fast, the subsequent evolution of large particles takes place on much longer time scales, over which it is necessary to take into account changing gas conditions. Our model assumes that turbulence is present throughout the entire phase of solids evolution. This point of view contrasts with the often-expressed opinion that turbulence decayed soon after the end of parent cloud collapse (Hayashi et al. 1985; Safronov, 1991). Only in the case when turbulence is exclusively associated with convection can one expect that a disk becomes laminar after particles with sizes $< 10^{-2}$ cm coagulate, making a disk transparent and stable against convection. For this to happen the coagulation process must be very efficient, leaving no small particles behind. However, infrared, optical, and near ultraviolet observation of T Tauri stars show the presence of accretion (see Bertout et al. 1988) for as long as there is evidence for a disk being present around a star. We may thus infer that protoplanetary disks maintain turbulence throughout their lifetimes. Such turbulence may be due to convection (if the process of small particles coagulation is inefficient), or may be the result of magnetorotational instability (Balbus & Hawley, 1991) or even purely rotational instability (Dubrulle, 1992). Therefore, in our opinion, a disk model with “generic” turbulence parameterized by constant α is a more realistic approximation of real protoplanetary disk than a laminar disk.

Besides being important for the evolution of the gas, the conclusions of turbulence has a direct consequences for dynamics of solid particles. By virtue of being coupled to the turbulent gas particles are subject to “pressure”, “viscosity”, and “diffusivity”. Obviously, the extent to which these effects are important depends on the effectiveness of gas-solids coupling. For example

⁵ As the name suggests, the minimum mass solar nebula concept was originally used to estimate the *total* minimum mass of the disk, which is a perfectly viable exercise. Later, however, this simple concept was extended (see for example Hayashi et al. 1985) to construct models of protoplanetary disks giving *radial* distribution of Σ , H , T , and ρ .

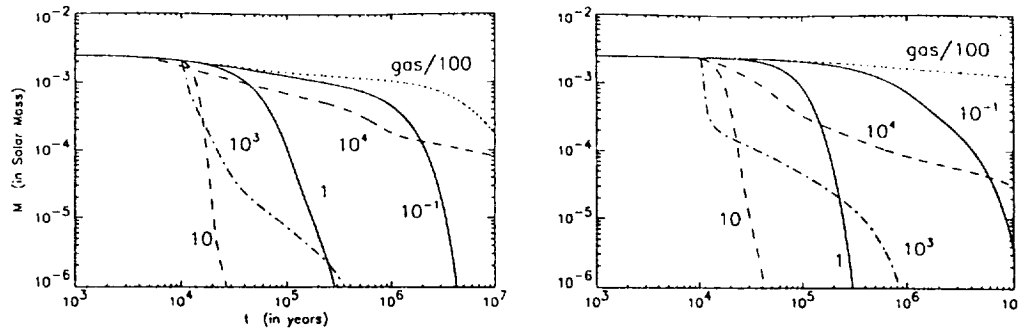


Fig. 6. Summary of solid particle evolution. The panels show the total mass of particles in the disk as a function of time: the left-hand panel corresponds to the evolutionary scenario with $\alpha = 0.01$, and the right-hand panel corresponds to the scenario with $\alpha = 0.001$. The correspondence between line styles and particle sizes is the same as in Figs. 5 and 6. In addition, lines are labeled by a number indicating particle size in cm.

the radial velocity of a 0.1 cm particle (which is well coupled to the gas) in an $\alpha = 0.01$ turbulent disk is about 2 orders of magnitude larger than the radial velocity of the same particle in a hypothetical quiescent disk characterized α -disk gas density and temperature. Other things being equal, the turbulent disk viscosity causes particle radial motion much larger than the radial motion of particle in a quiescent disk, which is exclusively due to the drag resulting from existence of the relative tangential velocity between a particle and the gas. Medium and large particles are less coupled to the gas and their radial velocities are dominated by the drag and not by turbulent viscosity.

Inspecting Fig. 6 we conclude that the total mass of $10 - 10^3$ cm particles drops below the total mass of solid material in the present-day solar system ($\sim 10^{-4} M_{\odot}$) on a time scale of about $10^4 - 10^5$ yr. Therefore, the coagulation time scale for particles of such sizes must be faster than 10^4 yr, otherwise there will be no material left to form the planets. Above we have estimated that $t_c \sim 10^4$ yr for 1 cm particles located at 10 AU after 10^5 yr from the beginning of our calculations. Extending this estimation for all 1 cm particles, we may conclude that they will increase their size and slow down before spiraling into the central star. However, the value of t_c is sensitive to all of the above assumptions, and the question of the solid matter survivability cannot be answered without including the coagulation process into our calculations.

Acknowledgements. This research was done while the authors were supported by the Lunar and Planetary Institute, which is operated by USRA under contract No. NASW-4574 with NASA. This is Lunar and Planetary Institute Contribution No. 867.

References

- Balbus, S.A. & Hawley, J.F. 1991, *ApJ*, 376, 214
 Beckwith, S.V.W. 1994, in *Theory of Accretion Disks - 2*, ed. W.J. Duschl, J. Frank, F. Meyer, E. Meyer-Hofmeister & W.M. Tscharnuter (Kulwer Academic Publishers), 1
 Bertout, C., Basri, G., Bouvier, J. 1988, *ApJ*, 330, 350
 Canuto, V.M. & Battaglia, A. 1988, *A&A*, 193, 313

- Cuzzi, J.N., Dobrovolskis, A.R., Champney, J.M. 1993, *Icarus*, 106, 102
 Dubrulle, B. 1992, *A&A*, 266, 592
 Dubrulle, B., Morfill, G., Starzik, M. 1995, *Icarus*, 114, 237
 Frank, J., King, A., Raine, D. 1985, in *Accretion Power in Astrophysics* (Cambridge University Press, Cambridge), 75
 Greenberg, R., Wacker, J.F., Hartmann, J.F., Chapman, C.R. 1978, *Icarus*, 35, 1
 Goldreich, P., Ward, W.R. 1973, *ApJ*, 183, 1051
 Hayashi, C., Nakazawa, K., Nakagawa, Y. 1985, in *Protostars & Planets II*, ed. D.C. Black & M.S. Matthews (Univ. of Arizona Press, Tucson), 1100
 Kaula, W.M. 1979, *Icarus*, 40, 262
 Levy, E.H. 1993, in *Planets around Pulsars*, ed. J.A. Phillips, S.E. Thorsett & S.R. Kulkarni (ASP Conf. Ser., 36), 181
 Morfill, G.E. 1988, *Icarus*, 75, 371
 Nakagawa, Y., Hayashi, C., Nakazawa, K. 1983, *Icarus*, 54, 361
 Pudritz, R.E., Norman, C.A., 1983, *ApJ*, 274, 677
 Reyes-Ruiz, M., Stepinski, T.F. 1995, *ApJ*, 438, 750
 Ruden, S.P., Pollack, J.B. 1991, *ApJ*, 375, 740
 Safranov, V.S. 1968, in: *Evolution of the Protoplanetary Cloud and the Formation of the Earth and Planets* (Nauka Press, Moscow)
 Safranov, V.S. 1991, *Icarus*, 94, 260
 Shakura, N.J., Sunyaev, R.A. 1973, *A&A*, 24, 337
 Strom, S.E., Edwards, S. 1993, in: *Planets around Pulsars*, ed. J.A. Phillips, S.E. Thorsett & S.R. Kulkarni (ASP Conf. Ser., 36), 235
 Weidenschilling, S.J. 1977, *MNRAS*, 180, 57
 Weidenschilling, S.J. 1988, in *Meteorites and the Early Solar System*, ed. J. Kerridge & M.S. Matthews (Univ. of Arizona Press, Tucson), 348
 Weidenschilling, S.J., Ruzmaikina, T.V. 1994, *ApJ*, 430, 713
 Wetherill, G.W. 1980, *ARA&A*, 18, 77

This article was processed by the author using Springer-Verlag L^AT_EX A&A style file version 3.